Proposal of Simplified Assessment Method for Surface Crack Growth Behavior under Creep-fatigue Condition

Isamu Nonaka* and Akira Nishikawa*

A simplified assessment method for surface crack growth behavior under creep-fatigue conditions was proposed. To verify this method, a series of experiments were performed. As a results, (1)this method proved to be useful in axial fatigue, axial creep-fatigue, bending fatigue and bending creep-fatigue. (2)In case of displacement holding, the average stress at the beginning of holding and at the end of holding proved to be suitable for this method. (3)In bending creep-fatigue, the crack was also observed at the back side surface of the plate.

INTRODUCTION

In order to estimate the structural integrity of elevated temperature components under creep-fatigue condition, it is necessary to clarify the creep-fatigue crack growth behavior. To estimate the behavior of surface crack without three-dimensional inelastic analysis, simplified estimation methods have been studied through bench mark, and some of them are presented to be feasible(1). However, it seems that there is some problems in order to apply them to the structural design.

The object of this study is to improve the applicability of a typical simplified estimation method. The method taken into account is based on R6 rule developed by CEGB in U.K.(2). The crack growth behavior under axial loads or bending loads are considered. From comparison of test results with estimations obtained by improved method, applicability and accuracy of the method are discussed.

Simplified Method to Predict Crack Growth Rate

*Ishikawajima-Harima Heavy Industries Co., Ltd.

First, the parameters to estimate the crack growth rate were investigated. As shown in Fig. 1, nonlinear fracture mechanics parameter, J-integral was calculated from the failure assessment diagram (FAD) in R6 rule(2). FAD shows the fracture criteria by using two parameter K_r and L_r. K_r is derived in option 2 of R6 rule by the equation:

$$K_r=\left\{\frac{E\varepsilon(L_r\sigma_y)}{L_r\sigma_y}+\frac{L_r^3\sigma_y}{2E\varepsilon(L_r\sigma_y)}\right\}^{-0.5} \quad \text{------- (1)}$$

Also K_r is derived in option 3 of R6 rule by the equation:

$$K_r=(J_e/J)^{0.5} \quad \text{------- (2)}$$

From Eq.(1) and Eq.(2), J-integral and modified J-integral J' which is the time differential of J-integral are described as follows:

$$J=\left\{\frac{E\varepsilon(L_r\sigma_y)}{L_r\sigma_y}+\frac{L_r^3\sigma_y}{2E\varepsilon(L_r\sigma_y)}\right\}\frac{K^2}{E} \quad \text{---(3)} \qquad J'=\frac{E}{E'}\varepsilon(L_r\sigma_y)\frac{K^2}{L_r\sigma_y} \quad \text{---(4)}$$

From Eq.(3) and Eq.(4), the estimation parameter of fatigue crack growth rate, ΔJ_f and that of creep-fatigue crack growth rate, ΔJ_c were described as follows. In creep-fatigue, $\Delta J_f+\Delta J_c$ should be used but only ΔJ_c was used here because ΔJ_f is negligible in many cases.

$$\Delta J_f=4\times J \quad \text{---(5)} \qquad \Delta J_c=J'\times t_H \quad \text{---(6)}$$

Secondly, as shown in Fig. 2, the crack growth rates were predicted based on the relationships between the crack growth rates and the parameters which were experimentally obtained for through cracks.

Verification Test

To verify the efficiency of the proposed method, a series of tests were conducted. Test conditions are shown in Table 1. Test material was Type 304 stainless steel. Specimens were plate with semi-circle surface notch. Temperatures were 550°C and 650°C. Loading patterns were axial fatigue, axial creep-fatigue, bending fatigue and bending creep-fatigue. Only axial fatigue was load controlled and other test conditions were displacement controlled. Fatigue wave form was triangular and creep-fatigue wave form was trapezoidal with 10 minutes hold. Crack growth rate was calculated from the crack front shape measured by the beach mark method and the electrical potential method.

Results and Discussion

Axial fatigue Fig. 3 shows the comparison of predictions with test results. Two kinds of load controlled tests were conducted. The predicted crack growth rate was nearly equal to the experimental one. Fig. 8(a) shows the fracture surface with beach mark.

Axial creep-fatigue Fig. 4 shows the comparison of predictions with test results. As the stress was not constant during displacement holding, the average stress at the beginning of holding and at the end of holding was used in the predictions. The predicted crack growth rate was nealy equal to the experimental one in one case but it was underestimated in the other case. Fig. 7 shows the simulated crack front shape based on the predictions. It was nearly equal to the beach mark.

Bending fatigue Fig. 5 shows the comparison of predictions with test results. The predicted crack growth rate was higher than the experimental one. This may be due to the overestimate of effective stress to extend the crack.

Bending creep-fatigue Fig. 6 shows the comparison of predictions with test results. The predicted crack growth rate was nearly equal to the experimental one. The fracture surface was shown in Fig. 8(d). The crack was also observed at the back side surface of the plate. It may be caused by the acceleration of crack initiation due to the creep damage accumulated during compressive holding.

Conclusion

The simplified assessment method for surface crack growth behavior under creep-fatigue conditions was proposed based on R6 rule. To verify this method, a series of the experiments were performed. The results were summarized as follows.

(1) Under both axial fatigue and bending creep-fatigue, the proposed crack growth rate was nearly equal to the experimental one. However under axial creep-fatigue the prediction was lower than the experiments at the small crack region while it was higher, at the large crack region. Also under bending fatigue the prediction was higher than the experiment.

(2) In case of displacement holding, the average stress at the beginning of holding and at the end of holding proved to be suitable for this method.

(3) In the bending creep-fatigue, the crack was also observed at the back side surface of the plate. It may be caused by the acceleration of crack initiation due to the creep damage accumulated during compressive holding.

References

(1) Iwasaki, R et al., Transaction of the 11th Int. Conf. on SMiRT L10/2, 1991, pp. 217-222.

(2) Milne I. et al., Int. J. of Pres. Ves. & Piping, Vol. 32, 1988, pp.3-104.

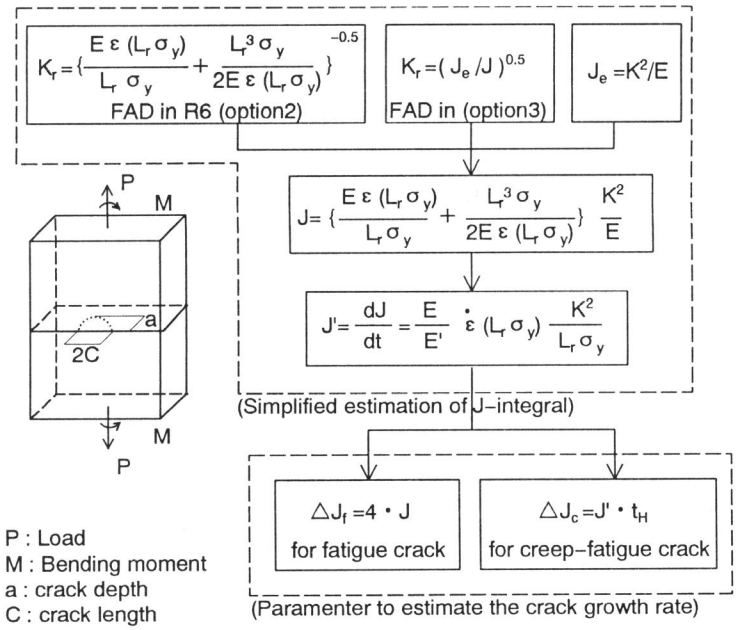

P : Load
M : Bending moment
a : crack depth
C : crack length

E : Young's modulus
E' : E'=E(for plane stress)
$E'=\frac{E}{1-\nu^2}$ (for plain strain)
ε : Strain obtained from cyclic $\sigma-\varepsilon$ equation
$\dot{\varepsilon}$: Creep strain rate
σ_y : 0.2% proof stress in cyclic $\sigma-\varepsilon$ equation
ν : Poisson's ratio
L_r : Collapse load ratio ($=\sigma/\sigma_y$)
J : J-integral
J' : Modified J-integral
J_e : Elastic J-integral
K : Stress intensity facter (Newman & Raju)
t_H : Creep hold time

Fig.1 Flow diagram to calculate the estimation parameter of crack growth rate.

Table 1 Test conditions.

Material	Temp.	Loading pattern	Control	Control value	P or δ
Type 304 stainless steel	550°C	Axial fatigue	Load	±147.1MPa	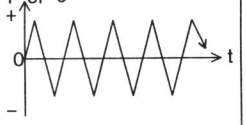
				±127.5MPa	
		Bending fatigue	Displacement*	±3.5mm	
	650°C	Axial creep-fatigue		±0.5mm	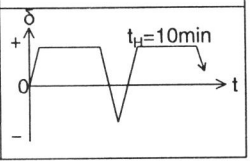
				±0.3mm	
		Bending creep-fatigue		±4.5mm	
				±7.0mm	

* Stroke between top grip and bottom grip.

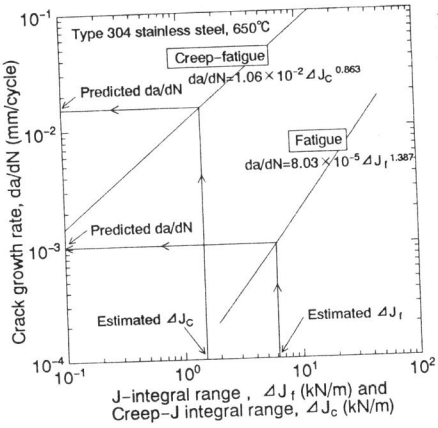

Fig.2 Prediction of crack growth rate based on Paris law of through crack.

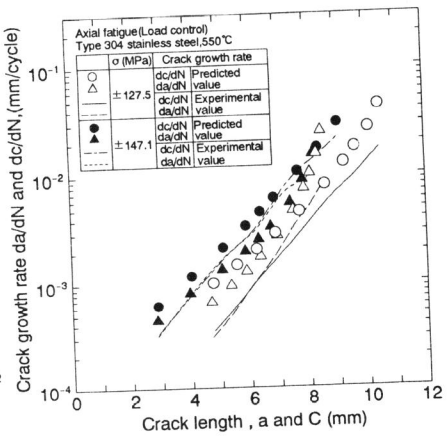

Fig.3 Comparision of the predicted crack growth rate with the experimental value in the axial fatigue.

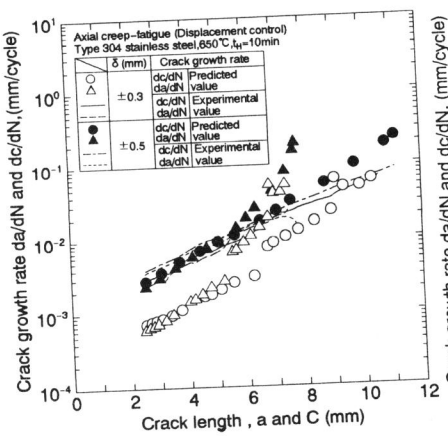

Fig.4 Comparison of the predicted crack growth rate with the experimental value in the axial creep-fatigue test.

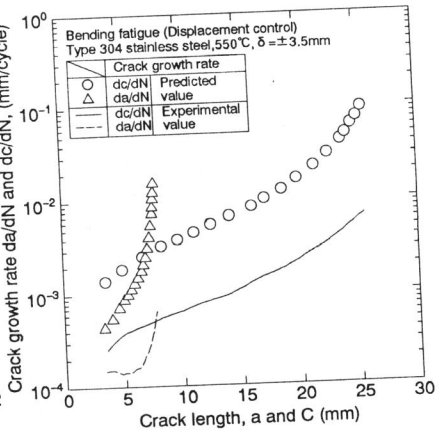

Fig.5 Comparison of the predicted crack growth rate with the experimental value in the bending fatigue test.

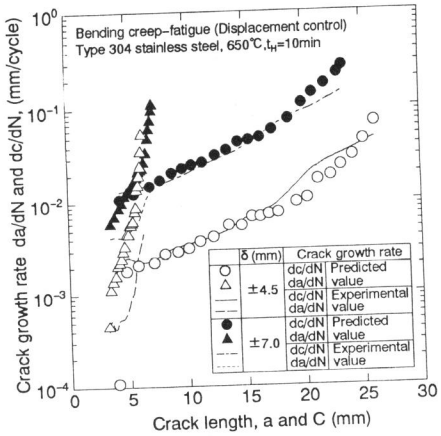

Fig.6 Comparison of the predicted crack growth rate with the experimental value in the bending creep-fatigue test.

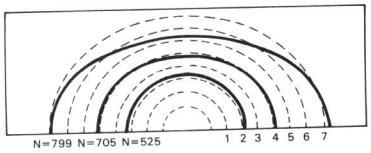

——Experimental crack front (Beach mark)
N=525, 705, 799cycles
------ Simulated crack front
1 N=465 cycles
2 N=712 cycles
3 N=837 cycles
4 N=894 cycles
5 N=916 cycles
6 N=923 cycles
7 N=925 cycles

Fig.7 An example of the simulated crack front shape in the axial creep-fatigue test.

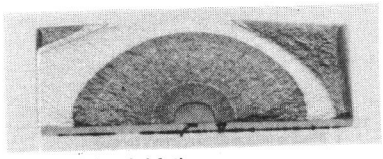

(a) axial fatigue

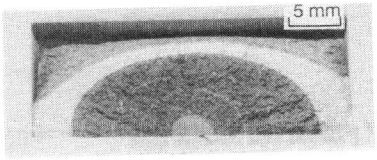

(b) axial creep-fatigue

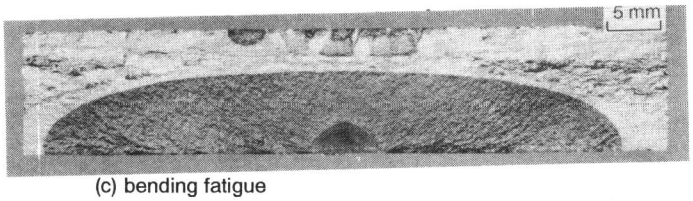

(c) bending fatigue

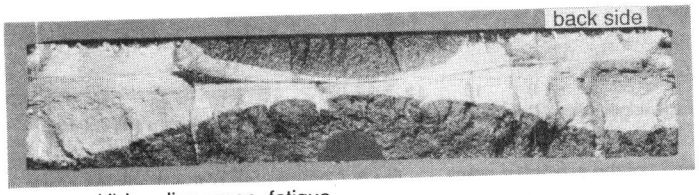

(d) bending creep-fatigue

Fig.8 Fracture surface of the specimen showing the beach mark.